THE JOURNAL OF PHYSICAL CHEMISTRY C

ARTICLE

pubs.acs.org/JPCC

Enhancing P3HT/TiO_2 Hybrid Photovoltaic Performance by Incorporating High Surface Potential Silica Nanodots into Hole Transport Layer

Jhih-Fong Lin,[†] Wei-Ben Wang,[§] Chun-Chih Ho,[†] Jwo-Huei. Jou,[§] Yang-Fang Chen,[‡] and Wei-Fang Su*[,†]

[†]Department of Material Science and Engineering and [‡]Department of Physics, National Taiwan University, No. 1, Sec. 4, Roosevelt Road, Taipei, 10617 Taiwan, R.O.C.

[§]Department of Material Science and Engineering, National Tsing Hua University, No. 101, Section 2, Kuang-Fu Road, Hsinchu, Taiwan 30013, R.O.C.

Supporting Information

ABSTRACT: We offer a novel approach to improve the performance of P3HT/TiO_2 hybrid photovoltaic devices by incorporating either hydroxyl- or amino-functionalized silica nanodots (SND−OH or SND−NH_2) into the hole transport layer of the PEDOT:PSS. The SNDs serve as screens between conducting polymer and ionomer PSS to improve the phase separation and charge transport of the PEDOT:PSS hole transport layer. The power conversion efficiency (PCE) was thus improved by 1.45 and 2.61 fold for devices fabricated with PEDOT:PSS containing 1 wt % of SND−OH (SND−OH device) and 1 wt % of SND−NH_2 (SND−NH_2 device), respectively, when compared with the devices fabricated by neat PEDOT:PSS. The increase in PCE arises from an increase in short circuit currents, which are affected by the phase separation of PEDOT:PSS with possessing incorporated SNDs. The low surface potential of hydroxyl-functionalized SNDs (SND−OH) is easily aggregated in the PEDOT:PSS solution and forms large-sized phase separation in the PEDOT:PSS film. The aggregation of SND−OH causes slight decreases in the resistance of PEDOT:PSS thin film from $(61 \pm 1$ to $69 \pm 4) \times 10^6$ Ohm/square and a decrease in the shielding effects of the SNDs. In contrast, the high surface potential of amino-functionalized SNDs are dispersed uniformly in the PEDOT:PSS solution and form morphologies with small-sized domains in the PEDOT:PSS film. As a result, the sheet resistance of PEDOT:PSS thin films is decreased from $(61 \pm 1$ to $46 \pm 3) \times 10^6$ Ohm/square. Therefore, the SND−NH_2 device exhibits greater performance over the SND−OH devices.

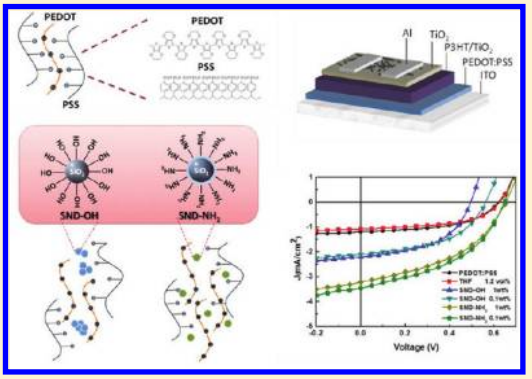

INTRODUCTION

Flexible electronics are of great interest because of their flexibility characteristics and their low processing costs. Soft materials such as organic or polymer materials play an important role in device fabrication. For organic light-emitting diodes, organic photovoltaic devices, and organic thin film transistors, conductive polymers are used as active materials and carrier transport layers.[1−10] Among the numerous conductive polymers, poly(3,4-ethylenedioxythiophene)/polystyrene sulfonic acid (PEDOT:PSS) is an important material in the creation of organic electronic devices because of its high conductivity and transparency. Commercial PEDOT:PSS is an aqueous dispersion, so many research groups have adopted a spin-casting process to fabricate thin films for investigation of its microstructure.

To date, the pancake microstructure model is the most accepted for PEDOT:PSS thin films.[11−18] Lang et al.[18] used high-angle annular dark field scanning TEM to correlate the relationship between the morphology and the elementary domain of the PEDOT:PSS thin films. They concluded that the spatial distribution of the PEDOT:PSS influences the carrier transport property of the film. Ionescu-Zanetti et al.[19] investigated the relationship between topography and corresponding current images of spin-casted PEDOT:PSS thin films. They report that the PEDOT and PSS lamella alternate in vertically directed regions of higher conductivity. Additionally, the step-like structure ensures that carriers can transport through the continuous domain of the PEDOT in a direction that is parallel to the surface. Using this pancake-like model, Nardes et al.[20] advanced the same structural model proposed by Lang et al. to explain the different transport mechanisms observed for both lateral and vertical directions within the PEDOT:PSS film.

Subsequently, many research groups found that incorporating an organic solvent[21−23] or salt[24] into the PEDOT:PSS aqueous solution could improve the conductivity of PEDOT:PSS thin films. They speculated that their organic solvents with large

Received: August 25, 2011
Revised: December 10, 2011
Published: December 20, 2011

dipole moments or ions that exhibit high binding energies interact with the electropositive PEDOT chain and electronegative PSS chain, respectively. This would induce a strong screening effect between the positively charged PEDOT and negatively charged PSS dopant. Therefore, the localization length of the PEDOT:PSS domain in the complex could be extended. This lowers the effective energy barrier for the charge carrier to hop between individual PEDOT grains. Unfortunately, these studies do not show the application of such highly conductive PEDOT:PSS thin films.[21−24] The correlation between conductivity of PEDOT:PSS thin films and the performance of such device has not been systematically investigated.

Previously, we demonstrated that the luminance of organic light-emitting diodes can be increased by 100% by using PEDOT:PSS that contained different functionalized silica nanodots (SNDs).[25,26] We speculate that the improvement results from the blocking and trapping effect of the various functionalized SNDs. Here we have incorporated different functionalized SNDs into the hole transport layer of PEDOT:PSS, improving the performance of P3HT/TiO_2 hybrid photovoltaic device. We systematically investigated the effects of different functionalized SNDs on the morphology and electrical properties of PEDOT:PSS thin films. We have thus deduced their relationship with the device's performance.

EXPERIMENTAL SECTION

All chemicals were purchased from Acros without purification. The SNDs were prepared by hydrolysis and condensation of sodium metasilicate according to the literature.[27] The resulting SNDs in tetrahydrofuran (THF) solution were ∼10 wt %, and the SND surface was capped with hydroxyl functional groups (SND−OH). We reacted (3-aminopropyl)-triethoxysilane (APTES) with the hydroxyl functional group of SND−OH to obtain amino-functionalized SNDs (SND−NH_2). First, we diluted the APTES to 0.1 wt % with THF; then, an APTES solution was mixed with the SND−OH solution by a volume ratio of 1:16. This mixture of APTES and SND−OH solution was then set for 24 h at 4 °C. A zeta potential analyzer (90Plus/BI-MAS, Brookhaven Instruments Corporation) was used to measure the surface potential of the SND−NH_2 to ensure complete surface modification.

To fabricate PEDOT:PSS thin films that are incorporated with different weight ratios of SNDs, the following procedure was used: First, the PEDOT:PSS solution (Baytron P VP AI 4083) was filtered through a 0.20 μm PVDF filter. This filtered solution was then blended with various weight ratios of two SNDs, respectively, to make two different PEDOT:PSS/SNDs solutions. A thin film of each PEDOT:PSS/SNDs was prepared by spin coating upon different types of substrate and then baked at 120 °C for 40 min. Atomic force microscopy (Digital Instruments, Nanoscopes III) was used to study the thin film's morphology. A four-point probe with a high-voltage source meter (Keithley model 2410) was used to measure the electrical properties of the different PEDOT:PSS/SNDs thin films.

The synthesis and surface modification of anatase TiO_2 nanorods was based on our previous report.[28] The conductive polymer P3HT was synthesized by Industrial Technology Research Institute of Taiwan; the molecular weight of P3HT is 65 kDa, and polydispersity (PDI) and regioregularity (RR) are 1.39 ± 0.06 and >95%, respectively.

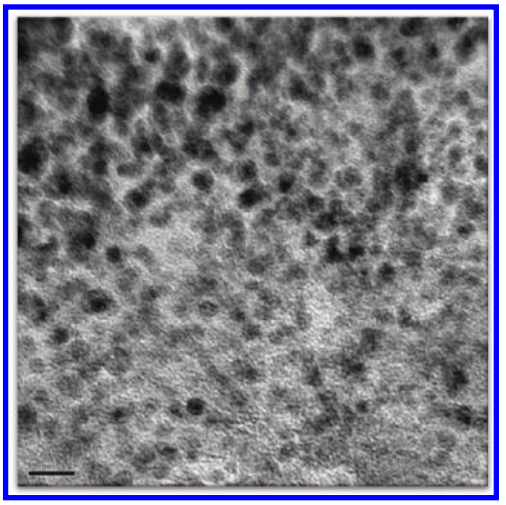

Figure 1. TEM image of as synthesized SND−OH.

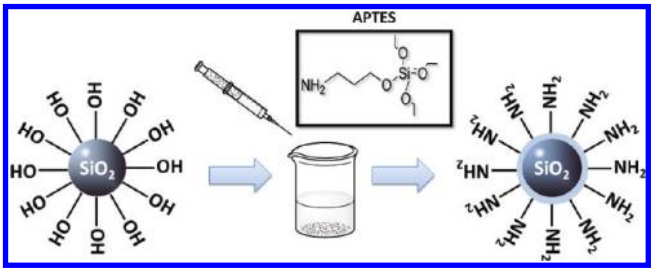

Figure 2. Schematic diagram of surface modification on SND−OH for producing SND−NH_2. The outer sphere around the SND−NH_2 is a monolayer of APTES.

To add PEDOT:PSS/SNDs into P3HT/TiO_2 photovoltaic devices so they will act as a hole transport layer, the following fabrication process was used: the PEDOT:PSS/SNDs thin film was spin coated onto a clean ITO glass at 5000 rpm for 1 min and then dried at 120 °C for 40 min. The photoactive layer was prepared by adding the hybrid solution of P3HT/TiO_2 nanorods with a weight ratio of 47:53 in the same manner as our previous study.[28] This hybrid solution was spin coated onto the PEDOT:PSS/SNDs thin film with the thickness of the photoactive layer around 120 nm. To reduce charge recombination at the interface between the active layer and the cathode, a ∼20 nm TiO_2 nanorods layer was deposited on the active layer to serve as a hole blocking layer. Next, the sample was stored in a glovebox for 1 day to remove the sample's solvent. Upon completion of the above steps, 100 nm of aluminum was deposited to use as the cathode. A solar simulator (Newport, model 66902) and voltage source meter (Keithley, model 2410) were used for device measurements.

RESULTS AND DISCUSSION

Figure 1 shows that the size of SND−OH is <10 nm when it was prepared by hydrolysis and condensation of sodium metasilicate.[25,27] The SND−NH_2 was synthesized by reacting the hydroxyl group of SND−OH with (3-aminopropyl)-triethoxysilane (APTES) as shown in Figure 2. Accordingly, the surface potential of SND−OH increased from −5 to +27 mV after surface modification. The surface potential of SND−NH_2 did not vary when added to an increasing amount of APTES in

Table 1. Compositions and Properties of Different PEDOT:PSS Thin Films

sample	type of nanodot[a]	SND (wt %)[b]	PEDOT:PSS (wt %)	roughness (nm)[c]	sheet resistance (10^6 ohm)
P		0	100.0	26	61 ± 1
THF		0	100.0	20	62 ± 2
O-0.1	SND−OH	0.1	99.9	22	67 ± 3
O-1	SND−OH	1.0	99.0	40	69 ± 4
N-0.1	SND−NH_2	0.1	99.9	27	62 ± 2
N-1	SND−NH_2	1.0	99.0	32	46 ± 3

[a] Surface potential of nanodot solution: SND−OH is −5 mV; SND−NH_2 is 27 mV. [b] THF is the solvent of nanodot solution and is evaporated off in the fabrication of PEDOT:PSS/SNDs thin film. The THF sample is prepared by adding the same amount of THF in the nanodot sample into the P sample as a control. [c] Roughness was determined by the atomic force microscopy.

SND−OH solution. This result indicates that the surface of SND−OH was completely modified by the APTES by placing an NH_2 group on the surface of the SNDs.

In this study, we used the four-point probe method to evaluate the electrical properties of different PEDOT:PSS thin films that contain different amount of either SND−OH or SND−NH_2. Recall that the SND−OH and SND−NH_2 were prepared in THF solution; when the nanodots were mixed with the PEDOT:PSS solution (to prepare different PEDOT:PSS/SNDs thin films), THF remained in solution, possibly affecting the preparation and final properties of the thin film. Therefore, we analyzed the films prepared using PEDOT:PSS solution both ±THF for proper comparison. Our results are summarized in Table 1. The PEDOT:PSS containing THF (THF sample) exhibits no significant differences in conductivity as compared with the neat PEDOT:PSS (P sample). However, for the samples containing SND−OH, their sheet resistances are somewhat higher than that of both PEDOT:PSS ± THF. The resistance of the PEDOT:PSS thin film increases slightly upon increasing the amount of SND−OH in the PEDOT:PSS. In contrast, samples containing SND−NH_2 exhibited an improved conductivity. The extent of enhancement is shown to increase with increasing amounts of SND−NH_2 in PEDOT:PSS. The different effects observed in the sheet resistance of the two nanodots on our PEDOT:PSS thin film may arise from the corresponding surface potential of either SND−OH or SND−NH_2. In the neat PEDOT:PSS aqueous solution, PEDOT and PSS associated with one another because of their opposing charges. The negatively charged PSS may help to enhance dispersion of PEDOT into the aqueous solution, thus improving the conductivity of the PEDOT polymer chain. Nardes et al.[20] concluded that the formation of a continuous and insulating PSS lamella structure in PEDOT:PSS thin film dramatically reduces the conductivity. Organic solvents[21−23] with high dipole moments such as dimethyl sulfoxide (DMSO) were added to the PEDOT:PSS to shield the attraction force between the positively charged PEDOT and negatively charged PSS dopants.[21−23] We have adapted this shielding mechanism produced by high dipole moment organic solvent and refer to it as "shielding effect" in this discussion of our study. This shielding effect allows for a more continuous transport path and thus decreases the probability of carrier hopping within the PEDOT:PSS thin film. To clarify the mechanism of

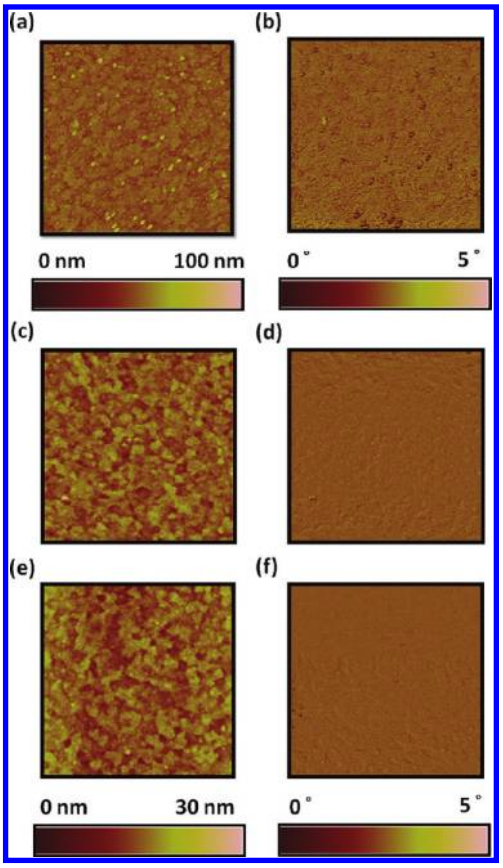

Figure 3. AFM topographic images and phase images, respectively, of (a,b) ITO substrate, (c,d) PEDOT:PSS/ITO substrate, and (e,f) PEDOT:PSS containing 1.2 vol % THF/ITO.

the observed sheet resistance changes in the films of PEDOT:PSS containing SNDs, we employed AFM to study the morphology of the films. We have thus established the relationship between morphology and electrical properties.

In organic photovoltaic devices, the PEDOT:PSS not only acts as the carrier's transport layer but also modifies the rough surface of ITO glass substrates. The presence of a PEDOT:PSS hole transport layer in the device can reduce possible charge recombination from direct contact between the active layer and the ITO electrode. The roughness of the ITO glass (Figure 3a) decreases from 53 to 26 nm after deposition of PEDOT:PSS upon the ITO glass (Figure 3c). The roughness of PEDOT:PSS on ITO was further reduced from 26 to 20 nm by incorporating THF into the PEDOT:PSS (Figure 3e). We have included the corresponding phase images for ITO, PEDOT:PSS/ITO, and PEDOT:PSS-THF/ITO in Figure 3b,d,f, respectively. The insets of Figure 4a−d show that there are no obvious differences in topography images among different PEDOT:PSS/SNDs samples. However, the surface roughness of the samples increased with increasing amounts of nanodots in the PEDOT:PSS. Furthermore, the extent of increase is much larger for our PEDOT:PSS/SND−OH samples as compared with that of the PEDOT:PSS/SND−NH_2 samples. (See Table 1 and Figure S1 of the Supporting Information.) To understand the differences in roughness among the different PEDOT:PSS/SNDs samples, phase images for the corresponding PEDOT:PSS/SNDs samples were also recorded. The phase images of two PEDOT:PSS/SNDs samples clearly show that the phase domain becomes more

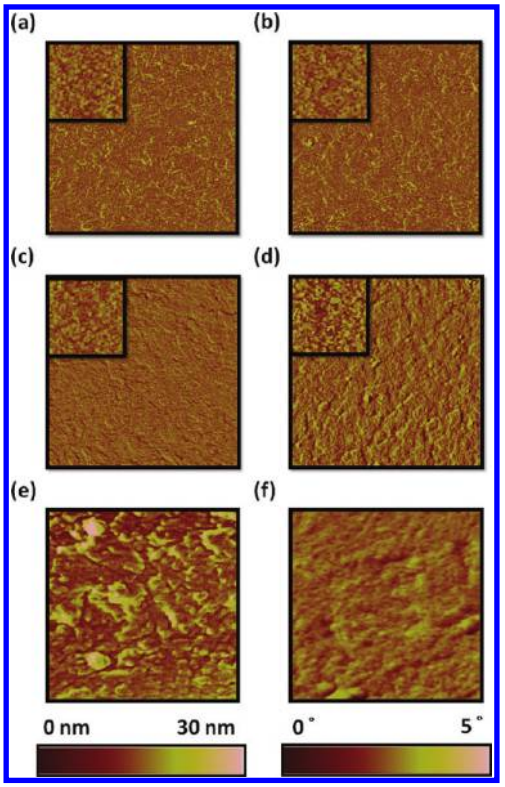

Figure 4. AFM phase images (5 μm × 5 μm) of PEDOT:PSS thin film incorporated with (a) 0.1 wt % SND−OH, (b) 1 wt % SND−OH, (c) 0.1 wt % SND−NH_2, and (d) 1 wt % SND−NH_2, and the large magnification AFM phase images (1 μm × 1 μm) of PEDOT:PSS thin film incorporated with (e) 1 wt % SND−OH or (f) 1 wt % SND−NH_2. The insets of panels a−d are AFM topographic images of corresponding samples.

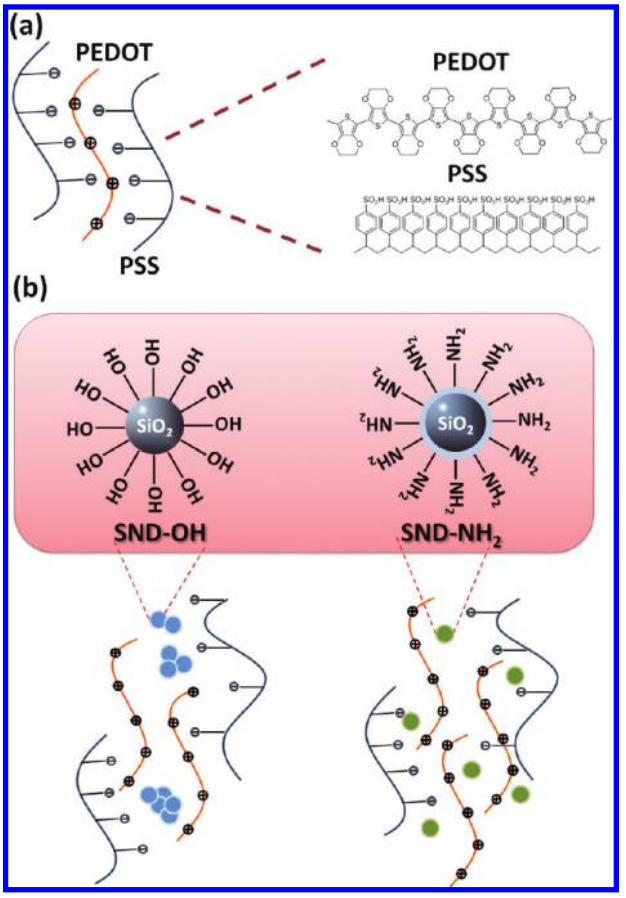

Figure 5. Schematic structure of PEDOT:PSS (a) before and (b) after incorporating SND−OH and SND−NH_2.

transparent with increasing amounts of SNDs (Figure 4a−d). These results indicate both SND−OH and SND−NH_2 can induce the phase separation between the conductive polymer PEDOT and the ionomer PSS. Consider the domain size in the AFM phase images: the SND−OH samples (Figure 4e) have larger domain sizes than that of the SND−NH_2 samples (Figure 4f). This feature may result from a small surface potential (−5 mV) of SND−OH, that allows easy aggregation in the PEDOT:PSS solution. This makes the phase domain larger than that of the SND−NH_2 samples. The large-sized SND−OH aggregate may become the center of carrier trapping and recombination, which explains the increased sheet resistance for samples prepared from PEDOT:PSS containing SND−OH. Furthermore, the small, granular structure observed in the phase images of the SND−NH_2 samples indicates that the SND−NH_2 can disperse well into the PEDOT:PSS solution and thus induce a stronger phase separation between the conductive polymer of PEDOT and the ionomer of PSS. As a result, the phase separation by SND−NH_2 forms a more continuous transport path that is composed of the conductive polymer PEDOT. It also reduces the probability of carrier trapping. Xia et al.[24] have found similar results regarding conductivity enhancement in PEDOT:PSS films when using different salt treatment. We suspect that the effect of SNDs with high surface potentials on the enhancement of conductivity is the same as that of charged metal ions. However, metal ions can become the center of charge trapping and erode the structure of the device. Because the SNDs have high surface potentials, they avoid these problems and are more suitable for use in the fabrication of organic photovoltaic devices. Furthermore, the differences in surface potential between SND−OH and SND−NH_2 not only influences the aggregation size and dispersion of the SNDs in solution but also affects the degree of phase separation in the PEDOT:PSS polymer complex. Therefore, the SND−OH samples exhibit a larger domain size and lower conductivity than that of the SND−NH_2 samples. The changes of phase separation due to incorporating different SNDs into PEDOT:PSS are sketched in Figure 5. For SND−OH samples, the low surface potential of SND−OH induces only weak phase separation between PEDOT and PSS. Therefore, this results in large SND−OH aggregations in the PEDOT:PSS films containing SND−OH. Notably, the SND−NH_2 with a high surface potential dispersed well and also effectively shielded the attractive force between the PEDOT and PSS in the PEDOT:PSS films containing SND−NH_2. Therefore, a smaller domain size was observed in the PEDOT:PSS containing SND−NH_2 thin film.

Finally, we compared the device performances of P3HT/TiO_2 hybrid photovoltaic device that incorporated either SND−OH or SND−NH_2 into the hole transport layer of the PEDOT:PSS. To exclude the effect of the THF solvent, we also fabricated a device using PEDOT:PSS containing THF as a reference control. Figure 6a is the I−V characteristics of the different devices, and Figure 6b illustrates the structure of the devices. The results of the device's performance are summarized in Table 2. We found that the performance of the device using PEDOT:PSS containing THF had no obvious change from that of the device using neat PEDOT:PSS. This indicates that THF functions only

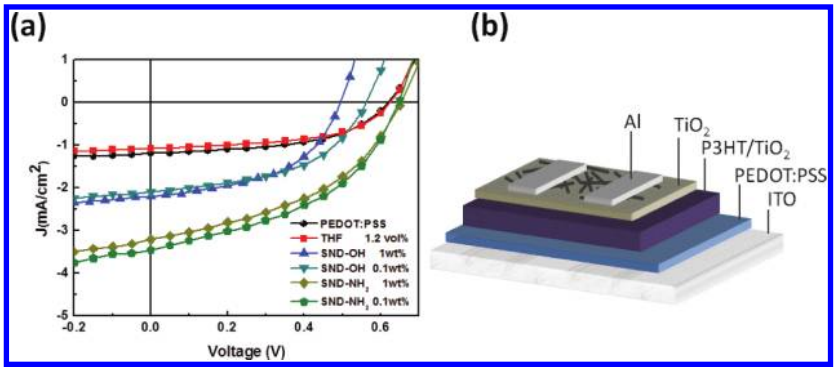

Figure 6. (a) $I-V$ curves of P3HT/TiO_2 photovoltaic devices with different additives in hole transport layer PEDOT:PSS under A.M.1.5 @ 100 mW/cm^2 illumination and (b) the structure of P3HT/TiO_2 photovoltaic device.

Table 2. Photovoltaic Properties of P3HT/TiO_2 Hybrid Devices Fabricated Using Different Hole Transport Layer

hole transport layer (HTL)	V_{OC} (V)	J_{SC} (mA/cm^2)	FF (%)	PCE (%)
P	0.62	1.19	51.41	0.38
THF	0.63	1.08	52.79	0.36
O-0.1	0.55	1.90	48.85	0.51
O-1	0.50	2.19	50.85	0.55
N-0.1	0.65	3.21	43.53	0.91
N-1	0.65	3.45	44.11	0.99

as a solvent and has no effect on the electrical property of the PEDOT:PSS. This is consistent with our above discussion on the electrical properties of different PEDOT:PSS film types (Table 1). On the other hand, there was a 45 and 160% improvement in power conversion efficiency (PCE) for the hole transport layer of PEDOT:PSS devices that contain either 1 wt % of SND−OH (SND−OH device) or SND−NH_2 (SND−NH_2 device), respectively, when compared with a device using neat PEDOT:PSS. Such improvement in device performance for PEDOT:PSS/SNDs samples mainly arises from the enhanced short circuit current density overran open circuit voltage and fill factor. We surmise that the SNDs in the PEDOT:PSS not only control phase separation between PEDOT and PSS but also are the recombination center as charge is transported through it. These two different mechanisms compete with each other during the operation of the device. Such competition results in the fill factor of the PEDOT:PSS/SND−NH_2 device falling only slightly due to well-dispersed SND−NH_2 in PEDOT:PSS. In contrast, the open circuit voltage and fill factor of the PEDOT:PSS/SND−OH device decreases due to the presence of the large SND−OH aggregates in the PEDOT:PSS. Interestingly, the presence of either SND−OH or SND−NH_2 in the PEDOT:PSS enhances the efficiency of charge injection of the P3HT/TiO_2 hybrid photovoltaic device. That means both SND−OH and SND−NH2 could induce phase separation between the PEDOT and PSS. Despite this, the extent of phase separation is affected by the surface potential and aggregated size of SNDs producing a differential improvement in device performance.

CONCLUSIONS

In summary, we offer a novel approach for improving the performance of P3HT/TiO_2 hybrid photovoltaic devices by incorporating functionalized SNDs into hole transport layer of PEDOT:PSS. Increasing the amount of SNDs can increase the extent of phase separation of PEDOT:PSS films. The domain size of PEDOT:PSS containing SND−NH_2 is smaller than that of SND−OH, causing an increase in the conductivity of PEDOT:PSS. To our PEDOT:PSS thin films, we added 1 wt % SNDs to serve as a hole transport layer in the device. Doing so increased thePCE from 0.38 to 0.55% and to 0.99% using SND−OH and SND−NH_2, respectively. The improvement mainly arise from increased short circuit current density, which makes us believe that the incorporation of SNDs enhances the carrier transport of the PEDOT:PSS layer in the P3HT/TiO_2 hybrid photovoltaic device.

ASSOCIATED CONTENT

Supporting Information. AFM topographic and phase contrast images of PEDOT:PSS thin film. This material is available free of charge via the Internet at http://pubs.acs.org.

AUTHOR INFORMATION

Corresponding Author

*E-mail: suwf@ntu.edu.tw. Tel: +886 2 33664078. Fax: +886 2 33664078.

ACKNOWLEDGMENT

We would like to thank the financial support from National Science Council of Taiwan (NSC 100-3113-E-002-012) for this research. We also like to thank Mr. An-Jey Su of Duquesne University, Pittsburgh, PA for his help with the language editing of this manuscript.

REFERENCES

(1) Burroughes, J. H.; Bradley, D. D. C.; Brown, A. R.; Marks, R. N.; Mackay, K.; Friend, R. H.; Burns, P. L.; Holmes, A. B. *Nature* **1990**, *347*, 539.

(2) Granstrom, M.; Petritsch, K.; Arias, A. C.; Lux, A.; Andersson, M. R.; Friend, R. H. *Nature* **1998**, *395*, 257.

(3) Peumans, P.; Uchida, S.; Forrest, S. R. *Nature* **2003**, *425*, 158.

(4) Yu, G.; Gao, J.; Hummelen, J. C.; Wudl, F.; Heeger, A. J. *Science* **1995**, *270*, 1789.

(5) Gustafsson, G.; Cao, Y.; Treacy, G. M.; Klavetter, F.; Colaneri, N.; Heeger, A. J. *Nature* **1992**, *357*, 477.

(6) Hains, A. W.; Liu, J.; Martinson, A. B. F.; Irwin, M. D.; Marks, T. J. *Adv. Funct. Mater.* **2010**, *20*, 595.
(7) Rider, D. A.; Worfolk, B. J.; Harris, K. D.; Lalany, A.; Shahbazi, K.; Fleischauer, M. D.; Brett, M. J.; Buriak, J. M. *Adv. Funct. Mater.* **2010**, *20*, 2404.
(8) Urban, J. J.; See, K. C.; Feser, J. P.; Chen, C. E.; Majumdar, A.; Segalman, R. A. *Nano Lett.* **2010**, *10*, 4664.
(9) Friedel, B.; Keivanidis, P. E.; Brenner, T. J. K.; Abrusci, A.; McNeill, C. R.; Friend, R. H.; Greenham, N. C. *Macromolecules* **2009**, *42*, 6741.
(10) Facchetti, A.; Luzio, A.; Musumeci, C.; Newman, C. R.; Marks, T. J.; Pignataro, B. *Chem. Mater.* **2011**, *23*, 1061.
(11) Greczynski, G.; Kugler, T.; Salaneck, W. R. *Thin Solid Films* **1999**, *354*, 129.
(12) Greczynski, G.; Kugler, T.; Keil, M.; Osikowicz, W.; Fahlman, M.; Salaneck, W. R. *J. Electron Spectrosc.* **2001**, *121*, 1.
(13) Crispin, X.; Marciniak, S.; Osikowicz, W.; Zotti, G.; Van der Gon, A. W. D.; Louwet, F.; Fahlman, M.; Groenendaal, L.; De Schryver, F.; Salaneck, W. R. *J. Polym. Sci., Part B: Polym. Phys.* **2003**, *41*, 2561.
(14) Kemerink, M.; Timpanaro, S.; de Kok, M. M.; Meulenkamp, E. A.; Touwslager, F. J. *J. Phys. Chem. B* **2004**, *108*, 18820.
(15) Ginger, D. S.; Pingree, L. S. C.; Reid, O. G. *Adv. Mater.* **2009**, *21*, 19.
(16) Snaith, H. J.; Kenrick, H.; Chiesa, M.; Friend, R. H. *Polymer* **2005**, *46*, 2573.
(17) Nardes, A. M.; Janssen, R. A. J.; Kemerink, M. *Adv. Funct. Mater.* **2008**, *18*, 865.
(18) Lang, U.; Muller, E.; Naujoks, N.; Dual, J. *Adv. Funct. Mater.* **2009**, *19*, 1215.
(19) Ionescu-Zanetti, C.; Mechler, A.; Carter, S. A.; Lal, R. *Adv. Mater.* **2004**, *16*, 385.
(20) Kemerink, M.; Nardes, A. M.; Janssen, R. A. J.; Bastiaansen, J. A. M.; Kiggen, N. M. M.; Langeveld, B. M. W.; van Breemen, A. J. J. M.; de Kok, M. M. *Adv. Mater.* **2007**, *19*, 1196.
(21) Ashizawa, S.; Horikawa, R.; Okuzaki, H. *Synth. Met.* **2005**, *153*, 5.
(22) Timpanaro, S.; Kemerink, M.; Touwslager, F. J.; De Kok, M. M.; Schrader, S. *Chem. Phys. Lett.* **2004**, *394*, 339.
(23) Park, S. M.; Lee, H. J.; Lee, J. *J. Phys. Chem. B* **2010**, *114*, 2660.
(24) Xia, Y.; Ouyang, J. *Macromolecules* **2009**, *42*, 4141.
(25) Jou, J. H.; Hsu, M. F.; Wang, W. B.; Liu, C. P.; Wong, Z. C.; Shyue, J. J.; Chiang, C. C. *Org. Electron.* **2008**, *9*, 291.
(26) Jou, J. H.; Wang, W. B.; Hsu, M. F.; Shyue, J. J.; Chiu, C. H.; Lai, I. M.; Chen, S. Z.; Wu, P. H.; Chen, C. C.; Liu, C. P.; Shen, S. M. *ACS Nano* **2010**, *4*, 4054.
(27) Hsu, Y. G.; Lin, K. H.; Chiang, I. L. *Mater. Sci. Eng., B* **2001**, *87*, 31.
(28) Chen, C. W.; Lin, Y. T.; Zeng, T. W.; Lai, W. Z.; Lin, Y. Y.; Chang, Y. S.; Su, W. F. *Nanotechnology* **2006**, *17*, 5781.